Available online at www.sciencedirect.com

SciVerse ScienceDirect

Ceramics International 39 (2013) 2375–2381

CERAMICS INTERNATIONAL

www.elsevier.com/locate/ceramint

A simple pathway in preparation of controlled porosity of biphasic calcium phosphate scaffold for dentin regeneration

Sarah Talib AbdulQader[a], Ismail Ab Rahman[a,*], Hanafi Ismail[b], Thirumulu Ponnuraj Kannan[a], Zuliani Mahmood[a]

[a]*School of Dental Sciences, Universiti Sains Malaysia, 16150 Kubang Kerian, Kelantan, Malaysia*
[b]*School of Materials and Minerals Resource Engineering, Universiti Sains Malaysia, 14300 Nibong Tebal, Penang, Malaysia*

Received 21 July 2012; received in revised form 30 August 2012; accepted 30 August 2012
Available online 11 September 2012

Abstract

A simple pathway in preparation of biphasic calcium phosphate scaffold of hydroxyapatite/beta-tricalcium phosphate with controlled pore size, shape and porosity using phosphoric acid and calcium carbonate was successfully developed. Microporosity was controlled by adjusting temperature and soaking time of the sintering process while macroporosity was obtained through addition of polyethylene spherical particles. The advantage of this method is that a highly pure biphasic calcium phosphate scaffold consisting of hydroxyapatite/beta-tricalcium phosphate in a controlled ratio of 20/80 with a mean pore size of 300 μm and 65% porosity can be produced. These properties of scaffold are of high potential for use in dentin regeneration.

Keywords: Biphasic calcium phosphate; Hydroxyapatite/Beta-tricalcium phosphate; Scaffold; Dentin regeneration

1. Introduction

Tissue engineering is a novel concept to regenerate functional new tissue using cells, bioactive molecules and scaffolds. A well-designed scaffold can provide a structural framework as well as a microenvironment to facilitate tissue formation [1,2]. Thus, the selection of appropriate scaffold parameters such as scaffold material, porosity, pore size, shape and pore distribution is critical in dentin tissue regeneration [3,4].

Biphasic calcium phosphate (BCP) materials have been reported as a suitable scaffold for hard tissue engineering [5–8]. BCPs consist of an intimate mixture of hydroxyapatite (HA) [$Ca_{10}(PO_4)_6(OH)_2$], and beta-tricalcium phosphate (β-TCP) [$Ca_3(PO_4)_2$] crystals of varying phase compositions (HA/β-TCP ratios) [9]. HA is bioactive and β-TCP is resorbable [10], and recent research has been devoted to manipulation of the composition of HA and β-TCP [11,12]. BCP of HA/β-TCP in a ratio of 20/80 has been reported as an appropriate scaffold material for bone tissue engineering and is more effective than pure HA or β-TCP alone [13] and also provided the best dentinogenic effects resulting in a thicker reparative dentin bridge and quicker formation of normal tubular dentin when it was placed in direct contact with pulp tissue [14]. Yıldırım et al. [15] reported that it served as an ideal calcium phosphate biomaterial to induce initial healing response and served as a good carrier for biologically active dentinogenic molecules.

Generally, there are two main methods to synthesize BCP: (1) sintering of calcium-deficient hydroxyapatite (CDHA) powder and (2) direct mechanical mixing of HA and β-TCP powders [16]. In the first method, a synthetic, natural or biological calcium-deficient hydroxyapatite (CDHA) [$Ca_{10-x}(PO_4)_{6-x}(HPO_4)x(OH)_{2-x}$] is sintered at a temperature above 700 °C. The extent of calcium deficiency (Ca/P molar ratio >1.67) determines the HA/β-TCP ratio in the BCP ceramics, which affects the reactivity of the material; the lower the ratio, the higher the reactivity. However, the reactivity also depends on particle

---

*Corresponding author. Tel.: +609 7675818; fax: +609 7642026.
E-mail address: arismail@usm.my (I.A. Rahman).

0272-8842/$ - see front matter
http://dx.doi.org/10.1016/j.ceramint.2012.08.089

size, and micro- and macro-porosity of the BCP that are affected by temperature and duration of sintering as well as by other variables of processing [9,17].

The intermediate product of CDHA in BCP processing is usually produced by the precipitation method [16,18]. In one type of precipitation method that employed $Ca(NO_3)_2$ and $(NH_4)_2HPO_4$ other phases of impurities resulted [19–21]. $Ca(OH)_2$ and H_3PO_4 were used in another precipitation process. However, the absorption of atmospheric CO_2 by $Ca(OH)_2$ and its partial transformation to $CaCO_3$ resulted in irreproducibility of BCP characteristics [9,22]. Hence, $CaCO_3$ was used due to its chemical stability during storage at standard conditions. The following reaction occurs between $CaCO_3$ and H_3PO_4 [9]:

$$(5-2x)CaCO_3+(3-x)H_3PO_4 \rightarrow (1-x)Ca_5(PO_4)_3 OH+xCa_3(PO_4)_2+(4-x)H_2O+(5-2x)CO_2 \quad (1)$$

$x = 10-6Ca/P; \quad 0 \le x \le 1$

In the case of direct mechanical mixing, the impurities in the initial commercial powders of HA and β-TCP affected the scaffold functional characteristics [16,17]. Another important factor that can also affect the functional characteristics of the scaffold is the porosity, in which pore size and total porous volume are very important. Microporosity (diameter $<10\ \mu m$) allows body fluid circulation, whereas macroporosity (diameter $>100\ \mu m$) provides a scaffold for cell attachment, migration, colonization and tissue deposition [23,24].

Many methods have been described for the preparation of macroporous scaffolds: use of polymeric sponges [25,26], porogen substances such as naphthalene particles [27], poly vinyl butyral (PVB) [28], polystyrene or polymethyl methacrylate beads [29], sodium chloride grains [30], flour [31] and gas-forming [32]. However, each technique has its own limitations and challenges. One of the serious challenges is controlling the total porosity, macropores shape and size. It was reported [33] that the total porosity of 65% was efficient compared to those of 25% and 75%, for total protein production and alkaline phosphatase (ALP) activity which were taken as indicators of growth/matrix production and for the comparison of cell differentiation. Tonomura et al. [5] concluded that the porous scaffold of 300 μm pore size was adequate for porcine dental pulp-derived cells to align with the scaffold surface, differentiate, and regenerate dentin-like tissue compared to granular and fiber-type scaffolds. Recently, Ando et al. [14] found that the transplanted dental pulp-derived cells using 2:8 ratio of HA/β-TCP of 300 μm pore size as a scaffold, regenerated dentin bridge-like structures on exposed dental pulp tissue. The hard tissue was positive for type I collagen (Col-1), osteonectin (ON), bone sialoprotein (BSP), and dentin sialoprotein (DSP), which are important markers for dentin.

The preparation of pure BCP scaffold with HA/β-TCP ratio of 20/80, controlled total porosity and macropores suitable for dentin regeneration has not been reported in the literature and hence the aim of this study was to develop a simple pathway for preparation of this material. The shape and size of the macropores were controlled by using a porogen, polyethylene (PE) spherical particles. Thermogravimetry analysis (TGA) and differential thermal analysis (DTA) were used to adjust thermal treatment during scaffold fabrication. Qualitative and quantitative X-ray diffraction (XRD), X-ray fluorescence spectroscopy (XRF) and fourier transform infrared (FTIR) were used for scaffold characterization. Pore size, shape and distribution were evaluated using a field emission scanning electron microscope (FESEM) and image analyzer. The total porosity was measured by the Archimedes method.

2. Materials and methods

2.1. BCP scaffold synthesis

BCP was processed by CDHA synthesis using the wet precipitation method. To prepare BCP of 20/80 ratio of HA/β-TCP, different Ca/P ratios were used. For whole ratios, H_3PO_4 (99.99%, Aldrich, USA) water solution was added at a rate of 7 mL/min into a water suspension of $CaCO_3$ ($\ge 99.0\%$, Aldrich, USA) under continuous stirring at room temperature (28 ± 3 °C). When the pH of the medium was 7.0 or 8.0, the mixture was heated at a temperature of 80 °C for an hour with stirring before cooling it down to room temperature. The precipitate was aged for 48 h, then washed three times and filtered using a centrifuge and dried using an oven at 100 °C for 24 h. The dried cake was crushed using pestle and mortar and the powder of mean particle size of 0.97 μm was mixed with PE spherical particles of 300–350 μm (Cosphere, USA) at a ratio of 4:2.5 v/v using alumina balls. The mixture was uniaxially pressed at 24 MPa in a 32 mm die to form 6 mm thick pellets.

To optimize the heating profile and to avoid cracks that form due to expansion of beads when heated in air, TGA–DTA analyses were performed on a mixture of CDHA/PE. The analysis was performed at a heating rate of 10 °C/min from 26 °C to 1000 °C. On the basis of TGA/DTA study, the pellets were fired at 400 °C for 2 h with 0.5 °C/min heating rate for PE removal and further sintered at 1000 °C for 2 h with 5 °C/min before cooling down to room temperature. Scaffold synthesis procedure is schematically illustrated in Fig. 1.

2.2. Characterization of the scaffold

The phase present and the ratio of HA/β-TCP of the scaffold were analyzed qualitatively and quantitatively by the XRD analysis using Eva and X'Pert HighScore Plus softwares, respectively. The scanning was done from 10° to 60° at a rate of 0.02°/min (Bruker, D2, PHASER) using Cu-Kα radiation generated at 30 kV and 10 mA. The crystalline phases were determined from a comparison of

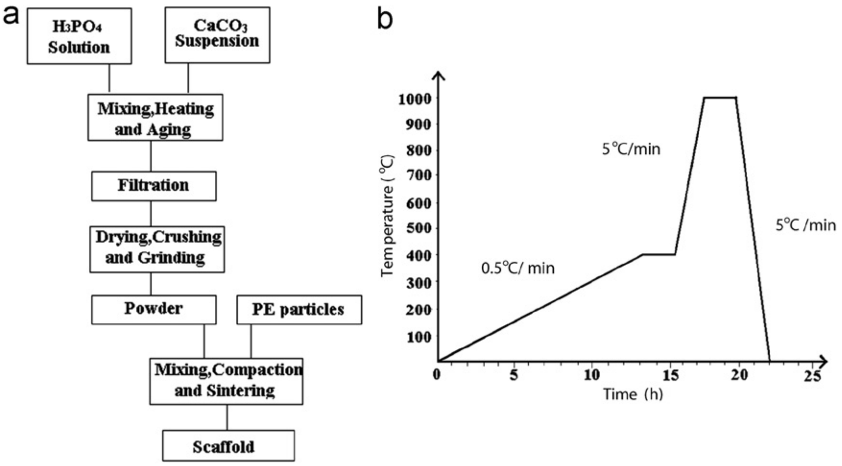

Fig. 1. Schematic presentation of (a) flow chart of BCP scaffold preparation procedure and (b) sintering program.

the registered patterns with the International Centre for Diffraction Data (ICDD) powder diffraction file (PDF).

Fourier transform infrared (FT-IR) spectrum (Perkin-Elmer 1720X) was obtained for a pellet of approximately 2 mg sample mixed with 800 mg ground spectroscopic-grade KBr that was analyzed in the diffuse reflectance mode over the wave number range of 400–4000 cm^{-1} with 4 cm^{-1} resolution. The chemical composition of the prepared BCP scaffold was measured by X-ray fluorescence spectroscopy (Rigaku, RIX 300).

Field emission scanning electron microscopy (FESEM, VPFESEMSUPRA, 35 VP) was used to evaluate the morphology of the PE particle, macro- and micro-porosity. The samples were first sputter-coated with a layer of platinum alloy (150 Å thick). The pore size was measured by using Image J software.

The shrinkage properties were analyzed to determine the shrinkage range of the pellets after sintering. The diameter of the porous pellet was measured before and after the sintering process using vernier caliper. The percentage of shrinkage was measured by the following equation [34]:

$$\%\ \text{Shrinkage} = (D_1 - D_2/D_1) \times 100 \tag{2}$$

where D_1 and D_2 are the diameters before and after sintering, respectively.

The Archimedes method using water was used to assess the total porosity of the scaffolds. This was performed by tying the scaffold by nylon string and weighing in air (M_{dry}) by an electronic balance (Precisa XT 220A). The sample was then placed in a beaker containing water in a vacuum glass container which was vacuumed to release the air from porosities of the sample for 1 h. While it submerged in the water (M_{sub}), the sample was weighed. The excess water on the surface of the sample was wiped by filter paper before the sample was weighed in air (M_{wet}). Measured values were used to calculate the porosity value with the following equation [35]:

$$\%\ \text{Porosity} = (M_{wet} - M_{dry})/(M_{wet} - M_{sub}) \times 100 \tag{3}$$

where M_{wet} is the wet mass, M_{dry} is the dry mass, and M_{sub} is the submerged mass.

3. Results and discussion

The parameters for the synthesis of BCP and the Ca/P ratio of the powders are summarized in Table 1. A pH of 7.0 or 8.0 was chosen for CDHA synthesis as it provides a neutral or slightly alkaline environment. This was in agreement with the results of the earlier researchers [16,36]. The qualitative XRD patterns for the synthesized BCP scaffolds of different ratios sintered at 1000 °C are shown in Fig. 2. The results showed that the prepared CDHA has a poor crystalline apatite structure, with peak positions matching closely with the diffraction peaks of stoichiometric hydroxyapatite (ICCD no. 00-0-9-0432), which is in agreement with earlier researchers [37,38]. The qualitative XRD patterns of the CDHA with Ca/P ratios of 1.50, 1.517, 1.534 and 1.55 at both pH values revealed that they were indistinguishable from each other (data not shown).

Fig. 2 shows the presence of the two phases in BCP samples: β-TCP [ICDD 01-070-2065] and HA [ICDD 00-009-0432] only. Three main peaks were observed for β-TCP at 2θ angle of 27.77°, 31.04° and 34.33° while for HA, they were observed at 31.86° and 33.05°. The highest peak intensities for β-TCP and HA were at 31.04° and 31.86° corresponding to the plane (0210) and (211), respectively. These peaks were considered as the most appropriate peaks for XRD analysis [11]. The results confirmed that the prepared BCP consisted of highly crystalline phases as indicated by the narrow and sharp diffraction peaks. This is in agreement with the work reported by earlier researchers [39,40].

The pH value clearly affected the final Ca/P ratios of BCP scaffolds as shown in Table 1. The higher the pH, the higher the HA percentage and subsequently, higher are the final Ca/P ratios. This may be due to the phase transformation of β-TCP to HA in alkaline environment by the

Table 1
The synthesis parameters, initial and final percentages of HA/β-TCP and Ca/P ratios of the BCP powder.

Samples	Theoretical phases (%)		Initial Ca/P ratio[a]	Final phases (%)[b]		Final Ca/P ratio[a]	Deviation (%)
	HA	β-TCP		HA	β-TCP		
pH 7							
A1	0	100	1.500	8.9	91.1	1.514	0.9
B1	10	90	1.517	20.1	79.9	1.535	1.2
C1	20	80	1.534	30.7	69.3	1.551	1.1
D1	30	70	1.550	39.2	60.8	1.565	1.0
pH 8							
A2	0	100	1.500	15.1	84.9	1.524	1.6
B2	10	90	1.517	25.6	74.4	1.542	1.6
C2	20	80	1.534	37.5	62.5	1.563	1.9
D2	30	70	1.550	47.7	52.3	1.579	1.9

[a] Calculated by Ca/P = wt% HA × 1.67 + wt% TCP × 1.50.
[b] Measured by quantitative XRD using X'Pert HighScore Plus software.

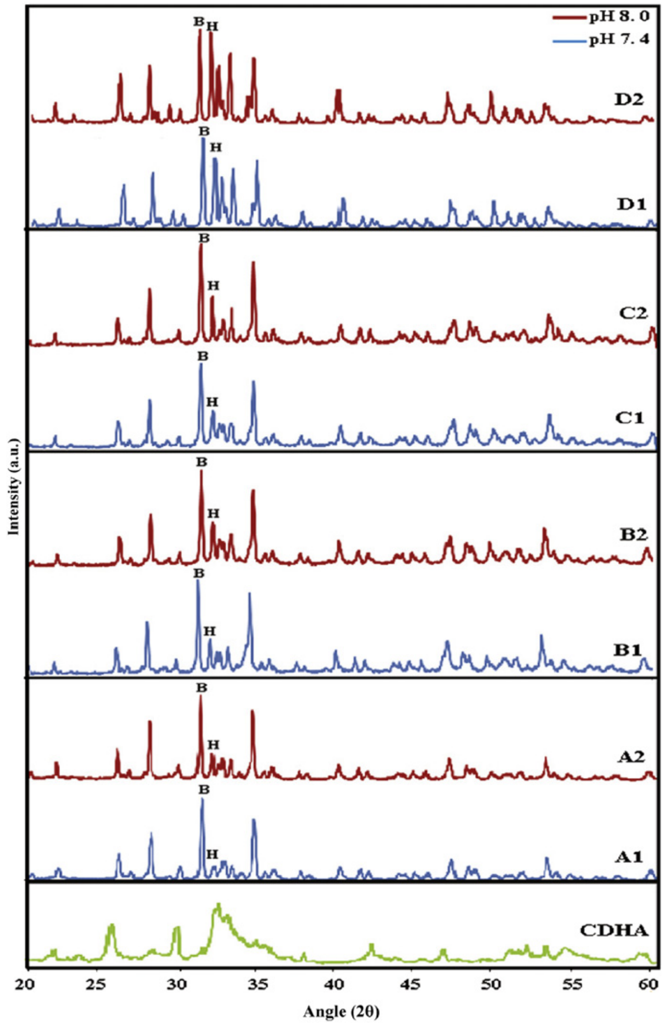

Fig. 2. Qualitative X-ray diffraction pattern of CDHA and different ratios of BCP scaffold synthesized at pH 7.0 or 8.0 and sintered at 1000 °C for 2 h (*B* = β-TCP, H = HA).

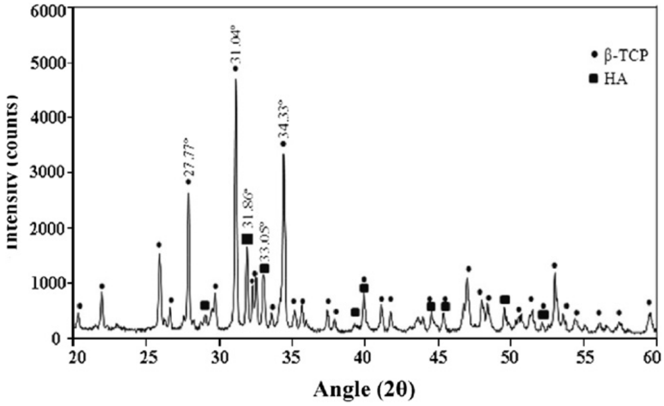

Fig. 3. Qualitative X-ray diffraction pattern of BCP scaffold of 1.517 Ca/P ratio synthesized at pH 7.0 and sintered at 1000 °C for 2 h.

following reaction [36]:

$$5Ca_3(PO_4)_2 + 3OH^- \rightarrow 3Ca_5(PO_4)_3OH + PO_4^{3-} \quad (4)$$

The results in Table 1 show that the deviation between initial and final Ca/P ratio is only ~1% for the samples prepared at pH 7.0 compared to those at pH 8.0 that leads to a variation of ~10 wt% of phase proportions after thermal treatment measured by quantitative XRD.

Based on theoretical calculation [41] using Eq. (5), Ca/P ratios of 1.534 and 1.517 result in HA/β-TCP of 20/80 and 10/90 respectively.

$$\text{Calculated Ca/P} = \text{wt\% HA} \times 1.67 + \text{wt\% TCP} \times 1.50 \quad (5)$$

Experimentally, a Ca/P ratio of 1.534 resulted in HA/β-TCP ratio of 30.7/69.3 instead of 20/80, while a Ca/P ratio of 1.517 resulted in HA/β-TCP ratio of 20.1/79.9 instead of 10/90. Therefore, Ca/P ratio of 1.517 at pH 7.0 was chosen to prepare 20/80 ratio of HA/β-TCP. Fig. 3 shows the qualitative X-ray diffraction pattern of BCP scaffold that contains only HA and β-TCP phases. However, the composition of the final powder did not depend directly on the Ca/P value of the initial reagents but rather depended strongly on the processing parameters such as, solution composition and supersaturation, temperature, pH, stirrer speed, duration and aging time that have been established. This synthesis condition achieved good reproducibility since the powders could be produced with a relative deviation of their Ca/P value ~1%. Thus, a simple pathway for the preparation of BCP was established.

For the BCP scaffold preparation using PE as a pore former, TGA/DTA thermograms of a mixture of CDHA/PE were performed. The results showed that the weight of the mixture decreased as temperature increased (Fig. 4). The first weight loss at ~100 °C is due to the evaporation of water. A sharp weight loss at ~300–380 °C is due to the burning out of PE particles. Thus, to ensure that the PE particles were burnt out completely and to avoid the cracks in the scaffold, the heating rate adopted was very slow at a sintering temperature below 400 °C. Other weight loss at temperatures above 750 °C is attributed to the decomposition of CDHA to HA and β-TCP according to the general reaction below [10,12,20].

$$\mathrm{Ca_{10-x}(HPO_4)_x(PO_4)_{6-x}(OH)_{2-x}} \xrightarrow{700\ ^\circ\mathrm{C}} (1-x)\mathrm{Ca_{10}(PO_4)_6(OH)_2} + 3x\mathrm{Ca_3(PO_4)_2} + x\mathrm{H_2O} \quad (6)$$

$$x = 10-6\mathrm{Ca/P}; \quad 0 \le x \le 1$$

Fig. 5 shows that BCP is composed of HA and β-TCP with no other phases. The characteristic peaks between 557–604 $\mathrm{cm^{-1}}$ and 945–1087 $\mathrm{cm^{-1}}$ were assigned to phosphate group ($\mathrm{PO_4^{3-}}$) and the peak at 3571 $\mathrm{cm^{-1}}$ was attributed to the stretching mode of hydroxyl group ($\mathrm{OH^-}$). The high peak intensity at about 1040 $\mathrm{cm^{-1}}$and the absence of absorbances at 1400–1600 $\mathrm{cm^{-1}}$ range and at about 875 $\mathrm{cm^{-1}}$ in the IR-spectrum confirm the absence of carbonate group ($\mathrm{CO_3^{2-}}$) indicating that the reaction of $\mathrm{CaCO_3}$/$\mathrm{H_3PO_4}$ system did not result in carbonated BCP. The results of this FTIR spectroscopy were in good agreement with those of the standard BCP infrared absorption spectrum [9,34].

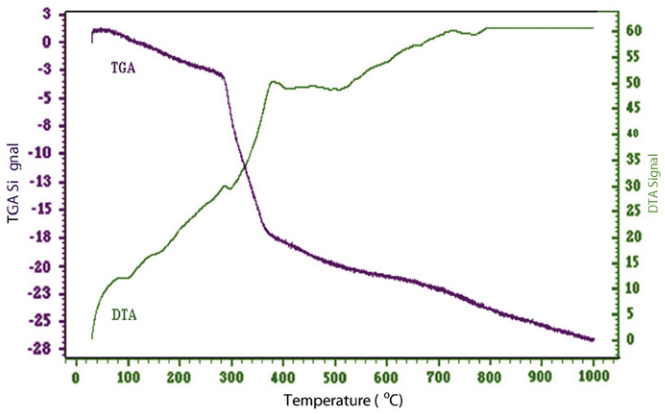

Fig. 4. TGA/DTA thermograms of a mixture of CDHA/PE.

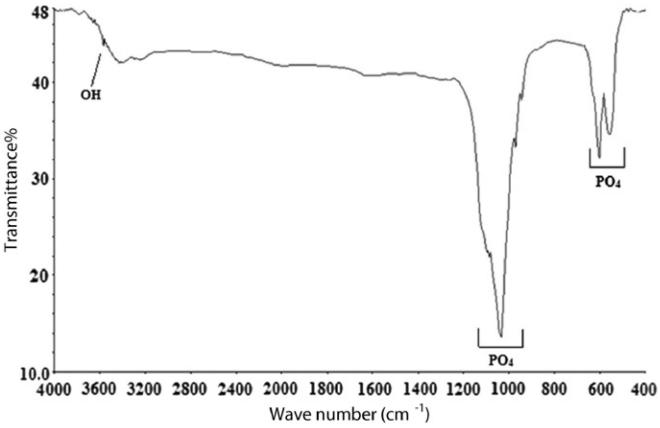

Fig. 5. FTIR spectrum of BCP scaffold of 1.517 Ca/P ratio synthesized at pH 7.0 and sintered at 1000 °C for 2 h.

The chemical composition of the prepared BCP was obtained by using XRF. The contents of CaO and $\mathrm{P_2O_5}$ were 57% and 43%, respectively. The results confirmed that the prepared BCP was pure without other compounds or impurities that may greatly affect the physical–chemical and consequently, the functional characteristics of the product.

The linear shrinkage of the sintered scaffold is calculated to be 9% by employing the formula (2) (in Section 2 of Materials and methods part). This can be attributed to the densification that occurs during the sintering process [36].

Fig. 6(a) shows the scaffold spherical macropores that were fabricated using spherical PE particles as porogens (Fig. 6(b)). The advantage of PE is that it creates a well-defined porosity with accurate pore size and can be easily eliminated by thermal treatment [4]. Statistical analysis of the scaffold macroporous structure revealed that the mean pore size was 308 ± 12 μm. The thermal removal of these porogens generated macropores with smaller size compared to the original size of porogen. This can be due to the scaffold shrinkage during the sintering process after the removal of PE particles.

The size of macropores is a critical factor affecting the supply of nutrition, cell attachment, migration, and tissue in-growth. For dentin tissue regeneration, odontoblasts, that are polarized cells, need to align on the surface of the matrix or existing dentin to generate dentin. The closed environment of porous scaffolds which is achieved by using spherical PE particles is beneficial for cell fate determination and induction of odontogenic differentiation.

A pore size of 300 μm was adequate for porcine dental pulp-derived cells to align with the surface and to regenerate dentin-like tissue [5].

Fig. 6(c) and (d) shows that the scaffold still had micropores. The presence of micropores can be attributed to the presence of HA phase. This result is in agreement with Descamps et al. [42] who reported that HA phase scattered in the matrix would act like an inhibitor of grain growth and enlargement of β-TCP, allowing a better densification of the material. It was found that the presence of

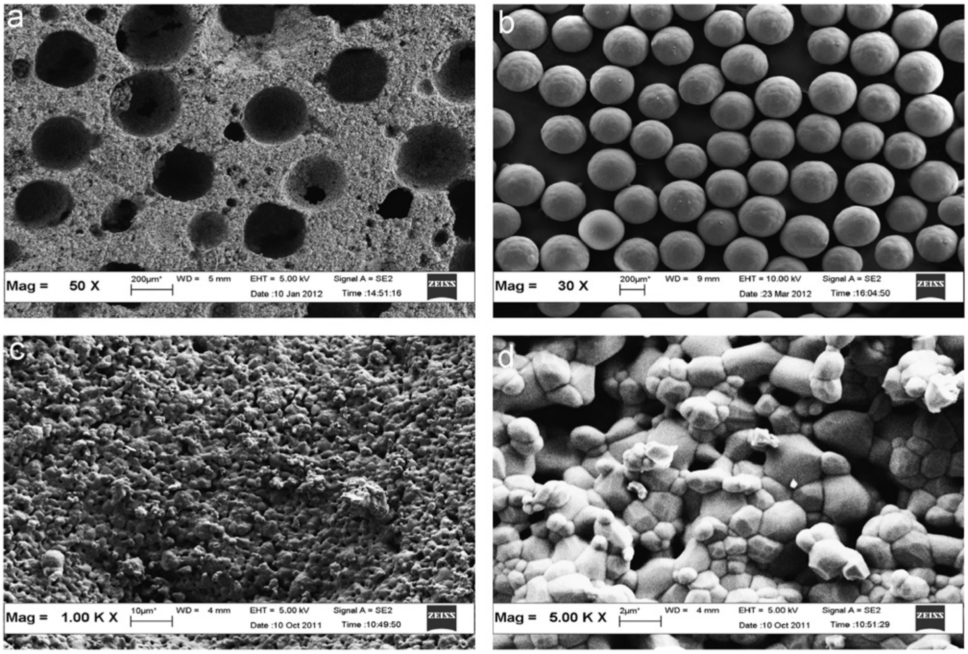

Fig. 6. SEM images showing (a) macroporosity, (b) PE particles, and (c) and (d) microporosity of BCP of 1.517 Ca/P ratio synthesized at pH 7.0 and sintered at 1000 °C for 2 h.

only 5% HA with micropore size of $<10\ \mu m$ could improve the densification properties of the ceramic. This depended on the sintering temperature and sintering program, which usually decrease with increase in temperature [43]. The micropores can be well preserved by adopting the sintering temperature and program used in this study. The presence of micropores in the scaffold is necessary for fluid circulation, vascularity restoration and for controlled delivery of drugs [44].

The total porosity of the prepared scaffold, as measured by the Archimedes method, was $64.62 \pm 0.84\%$. It is considered as a total porous volume in the scaffold which includes both micropores and macropores volume. This percentage is beneficial for protein production and ALP activity, which are necessary for the differentiation of cells [33].

4. Conclusions

In this study, a simple and reproducible pathway for producing highly pure BCP scaffold of HA/β-TCP in a ratio of 20/80 with 65% total porosity and $300\ \mu m$ spherical shape macropores, besides the preservation of the micropores structure has been successfully developed. The scaffold was produced by using $CaCO_3$ and H_3PO_4 as the starting materials with Ca/P deviation of only ~1% at pH 7.0. The presence of micropores is very helpful for the flow of nutrients, while the controlled macropores shape with a mean size of $300\ \mu m$ is suitable for the alignment of dental pulp-derived cells and its differentiation to odontoblasts. Hence, this porous BCP scaffold holds promise to be used in dentine tissue regeneration.

Acknowledgments

The authors would like to thank the Universiti Sains Malaysia for funding this research through the RU Grant no. 001/PPSG/814110.

References

[1] M. Nakashima, A. Akamine, The application of tissue engineering to regeneration of pulp and dentin in endodontics, Journal of Endodontics 31 (2005) 711–718.

[2] S.E.D.M. Saber, Tissue engineering in endodontics, Journal of Oral Science 51 (2009) 495–507.

[3] D. Tziafas, O. Pantelidou, A. Alvanou, G. Belibasakis, S. Papadimitriou, The dentinogenic effect of mineral trioxide aggregate (MTA) in short-term capping experiments, International Endodontic Journal 35 (2002) 245–254.

[4] E. Chevalier, D. Chulia, C. Pouget, M. Viana, Fabrication of porous substrates: a review of processes using pore forming agents in the biomaterial field, Journal of Pharmaceutical Sciences 97 (2008) 1135–1154.

[5] A. Tonomura, D. Mizuno, A. Hisada, N. Kuno, Y. Ando, Y. Sumita, M.J. Honda, K. Satomura, H. Sakurai, M. Ueda, Differential effect of scaffold shape on dentin regeneration, Annals of Biomedical Engineering 38 (2010) 1664–1671.

[6] L. Zhang, N. Hanagata, M. Maeda, T. Minowa, T. Ikoma, H. Fan, X. Zhang, Porous hydroxyapatite and biphasic calcium phosphate ceramics promote ectopic osteoblast differentiation from mesenchymal stem cells, Science and Technology of Advanced Materials 10 (2009) 025003.

[7] E. Lerouxel, P. Weiss, B. Giumelli, A. Moreau, P. Pilet, J. Guicheux, P. Corre, J.M. Bouler, G. Daculsi, O. Malard, Injectable calcium phosphate scaffold and bone marrow graft for bone reconstruction in irradiated areas: an experimental study in rats, Biomaterials 27 (2006) 4566–4572.

[8] L.T. Lee, P.C. Kwan, Y.F. Chen, Y.K. Wong, Comparison of the effectiveness of autologous fibrin glue and macroporous biphasic

calcium phosphate as carriers in the osteogenesis process with or without mesenchymal stem cells, Journal of the Chinese Medical Association 71 (2008) 66–73.

[9] Z. Zyman, M. Tkachenko, D. Polevodin, Preparation and characterization of biphasic calcium phosphate ceramics of desired composition, Journal of Materials Science: Materials in Medicine 19 (2008) 2819–2825.

[10] S.C. Wu, H.C. Hsu, S.K. Hsu, W.H. Wang, W.F. Ho, Preparation and characterization of four different compositions of calcium phosphate scaffolds for bone tissue engineering, Materials Characterization 62 (2011) 526–534.

[11] S. Raynaud, E. Champion, D. Bernache-Assollant, J.P. Laval, Determination of calcium/phosphorus atomic ratio of calcium phosphate apatites using X-ray diffractometry, Journal of the American Ceramic Society 84 (2001) 359–366.

[12] S.V. Dorozhkin, Calcium orthophosphates: occurrence, properties, biomineralization, pathological calcification and biomimetic applications, Biomatter 1 (2011) 121–164.

[13] T.L. Arinzeh, T. Tran, J. Mcalary, G. Daculsi, A comparative study of biphasic calcium phosphate ceramics for human mesenchymal stem-cell-induced bone formation, Biomaterials 26 (2005) 3631–3638.

[14] Y. Ando, M.J. Honda, H. Ohshima, A. Tonomura, T. Ohara, T. Itaya, H. Kagami, M. Ueda, The induction of dentin bridge-like structures by constructs of subcultured dental pulp-derived cells and porous HA/TCP in porcine teeth, Nagoya Journal of Medical Science 71 (2009) 51–62.

[15] S. Yıldırım, A. Alacam, Z.K. Sarıtas, T. Oygür, In vivo effect of calcium phosphate biomaterials on dog dental pulp, Biotechnology and Biotechnological Equipment 21 (2007) 198–204.

[16] R. LeGeros, S. Lin, R. Rohanizadeh, D. Mijares, J. LeGeros, Biphasic calcium phosphate bioceramics: preparation, properties and applications, Journal of Materials Science: Materials in Medicine 14 (2003) 201–209.

[17] S.V. Dorozhkin, Biphasic, triphasic and multiphasic calcium orthophosphates, Acta Biomaterialia 8 (2012) 963–977.

[18] Z. Zyman, D. Rokhmistrov, I. Ivanov, M. Epple, The influence of foreign ions on the crystal lattice of hydroxyapatite upon heating, Materialwissenschaft Und Werkstofftechnik 37 (2006) 530–532.

[19] T.W. Kim, Y.M. Park, D.H. Kim, H.H. Jin, K.K. Shin, J.S. Jung, H.C. Park, S.Y. Yoon, In situ formation of biphasic calcium phosphates and their biological performance in vivo, Ceramics International 38 (2012) 1965–1974.

[20] S. Raynaud, E. Champion, D. Bernache-Assollant, P. Thomas, Calcium phosphate apatites with variable Ca/P atomic ratio I. Synthesis, characterisation and thermal stability of powders, Biomaterials 23 (2002) 1065–1072.

[21] C. Ergun, Z. Evis, T.J. Webster, F.C. Sahin, Synthesis and microstructural characterization of nano-size calcium phosphates with different stoichiometry, Ceramics International 37 (2011) 971–977.

[22] M. Akao, H. Aoki, K. Kato, A. Sato, Dense polycrystalline b-tricalcium phosphate for prosthetic applications, Journal of Materials Science 17 (1982) 343–346.

[23] T. Abdurrahim, I. Sopyan, Recent progress on the development of porous bioactive calcium phosphate for biomedical applications, Recent Patents on Biomedical Engineering 1 (2008) 213–229.

[24] T. Thamaraiselvi, S. Rajeswari, Biological evaluation of bioceramic materials-a review, Trends in Biomaterials and Artificial Organs 24 (2004) 172.

[25] Y.K. Jun, W.H. Kim, O.K. Kweon, S.H. Hong, The fabrication and biochemical evaluation of alumina reinforced calcium phosphate porous implants, Biomaterials 24 (2003) 3731–3739.

[26] C. Wu, J. Chang, W. Zhai, S. Ni, J. Wang, Porous akermanite scaffolds for bone tissue engineering: preparation, characterization, and in vitro studies, Journal of Biomedical Materials Research Part B: Applied Biomaterials 78 (2006) 47–55.

[27] J. Lu, B. Flautre, K. Anselme, P. Hardouin, A. Gallur, M. Descamps, B. Thierry, Role of interconnections in porous bioceramics on bone recolonization in vitro and in vivo, Journal of Materials Science: Materials in Medicine 10 (1999) 111–120.

[28] D.M. Liu, Fabrication of hydroxyapatite ceramic with controlled porosity, Journal of Materials Science: Materials in Medicine 8 (1997) 227–232.

[29] A. Uchida, S. Nade, E. McCartney, W. Ching, Bone ingrowth into three different porous ceramics implanted into the tibia of rats and rabbits, Journal of Orthopaedic Research 3 (1985) 65–77.

[30] L. Olah, K. Filipczak, Z. Jaegermann, T. Czigany, L. Borbas, S. Sosnowski, P. Ulanski, J.M. Rosiak, Synthesis, structural and mechanical properties of porous polymeric scaffolds for bone tissue regeneration based on neat poly (ε-caprolactone) and its composites with calcium carbonate, Polymers for Advanced Technologies 17 (2006) 889–897.

[31] A. Slosarczyk, J. Szymura-Oleksiak, B. Mycek, The kinetics of pentoxifylline release from drug-loaded hydroxyapatite implants, Biomaterials 21 (2000) 1215–1221.

[32] J. Saggio-Woyansky, C.E. Scott, W. Minnear, Processing of porous ceramics, American Ceramic Society Bulletin 71 (1992) 1674–1682.

[33] P. Kasten, I. Beyen, P. Niemeyer, R. Luginbu, M. Bohner, W. Richter, Porosity and pore size of b-tricalcium phosphate scaffold can influence protein production and osteogenic differentiation of human mesenchymal stem cells: an in vitro and in vivo study, Acta Biomaterialia 4 (2008) 1904–1915.

[34] L.I. Shihong, J.R. de Wijn, L.I. Jiaping, L. Pierre, K. de Groot, Macroporous biphasic calcium phosphate scaffold with high permeability/porosity ratio, Tissue Engineering 9 (2003) 535–548.

[35] L. Lin, S. Ju, L. Cen, H. Zhang, Q. Hu, Fabrication of porous b-TCP scaffolds by combination of rapid prototyping and freeze drying technology, in: X.W. Yi Peng (Ed.), in: APCMBE, IFMBE Proceedings, vol. 19, Springer-Verlag, Berlin Heidelberg, 2008, pp. 88–91.

[36] A. Krajewski, A. Ravaglioli, R. Barbucci, Bioceramics and biological glasses, in: R. Barbucci (Ed.), Integrated Biomaterials Science, Springer, US, New York, 2002, pp. 189–254.

[37] S.C. Liou, S.Y. Chen, Transformation mechanism of different chemically precipitated apatitic precursors into [beta]-tricalcium phosphate upon calcination, Biomaterials 23 (2002) 4541–4547.

[38] S.C. Liou, S.Y. Chen, H.Y. Lee, J.S. Bow, Structural characterization of nano-sized calcium deficient apatite powders, Biomaterials 25 (2004) 189–196.

[39] G. Daculsi, Biphasic calcium phosphate concept applied to artificial bone, implant coating and injectable bone substitute, Biomaterials 19 (1998) 1473–1478.

[40] R.W.N. Nilen, P. Richter, The thermal stability of hydroxyapatite in biphasic calcium phosphate ceramics, Journal of Materials Science: Materials in Medicine 19 (2008) 1693–1702.

[41] M. Vallet-Regi, L. Rodriguez-Lorenzo, A. Salinas, Synthesis and characterisation of calcium deficient apatite, Solid State Ionics 101 (1997) 1279–1285.

[42] M. Descamps, J. Hornez, A. Leriche, Effects of powder stoichiometry on the sintering of [beta]-tricalcium phosphate, Journal of the European Ceramic Society 27 (2007) 2401–2406.

[43] O. Petrov, E. Dyulgerova, L. Petrov, R. Popova, Characterization of calcium phosphate phases obtained during the preparation of sintered biphase Ca–P ceramics, Materials Letters 48 (2001) 162–167.

[44] K. Jasadee, K. Lupong, Properly engineered ceramic scaffolds for sustained drug delivery, Journal of Material Science and Engineering 4 (2010) 34.